Probing the Basis of Domain-Dependent Inhibition Using Novel Ketone Inhibitors of Angiotensin-Converting Enzyme[†,‡]

Jean M. Watermeyer, Wendy L. Kröger, Hester G. O'Neill, B. Trevor Sewell, and Edward D. Sturrock*

Division of Medical Biochemistry, Institute of Infectious Disease and Molecular Medicine, University of Cape Town, Observatory 7925, South Africa

Received February 14, 2008; Revised Manuscript Received April 2, 2008

ABSTRACT: Human angiotensin-converting enzyme (ACE) has two homologous domains, the N and C domains, with differing substrate preferences. X-ray crystal structures of the C and N domains complexed with various inhibitors have allowed identification of active site residues that might be important for the molecular basis of this selectivity. However, it is unclear to what extent the different residues contribute to substrate domain selectivity. Here, cocrystal structures of human testis ACE, equivalent to the C domain, have been determined with two novel C domain-selective ketomethylene inhibitors, (5*S*)-5-[(*N*-benzoyl)amino]-4-oxo-6-phenylhexanoyl-L-tryptophan (kAW) and (5*S*)-5-[(*N*-benzoyl)amino]-4-oxo-6-phenylhexanoyl-L-phenylalanine (kAF). The ketone groups of both inhibitors bind to the zinc ion as a hydrated geminal diolate, demonstrating the ability of the active site to catalyze the formation of the transition state. Moreover, active site residues involved in inhibitor binding have been mutated to their N domain counterparts, and the effect of the mutations on inhibitor binding has been determined. The C domain selectivity of these inhibitors was found to result from interactions between bulky hydrophobic side chain moieties and C domain-specific residues F391, V518, E376, and V380 (numbering of testis ACE). Mutation of these residues decreased the affinity for the inhibitors 4−20-fold. T282, V379, E403, D453, and S516 did not contribute individually to C domain-selective inhibitor binding. Further domain-selective inhibitor design should focus on increasing both the affinity and selectivity of the side chain moieties.

The existence of two homologous active sites in one polypeptide chain is a rare phenomenon, thought to be caused by gene duplication leading to the development of new activities (*1, 2*). Human somatic angiotensin-converting enzyme (ACE)[1] is one such case, having two 55% identical domains, N and C, each containing an active site with a zinc binding motif, HEMGH (*3, 4*). ACE is a key target for the treatment of hypertension because of its role in increasing blood pressure via the renin-angiotensin system (*5, 6*).

Further examples of such two-domain enzymes are sucrase-isomaltase (SI) and lactase-phlorizin hydrolase (LPH), both involved in sugar metabolism (*7, 8*). In these enzymes, the homologous domains, which are ∼40% identical, bind similar but distinct substrates. The domains of SI cleave related disaccharides sucrose and isomaltose, while LPH cleaves lactose and the glucoside phlorizin. In the case of LPH, mechanism-based domain-selective inhibitors were used to elucidate the activities of the two domains (*9*). Other examples of enzymes containing homologous active domains include adenylyl transferase of *Escherichia coli* (*10*), which catalyzes the adenylylation and deadenylylation of glutamine synthetase, and protein disulfide isomerase (*11*), which catalyzes disulfide bond oxidation, reduction, and isomerization.

In all of these examples, a few active site substitutions correspond to significantly different, but functionally complementary, substrate specificities for the homologous domains. ACE differs from these enzymes in that its activity is not highly specific, with each domain being able to cleave a range of peptide sequences; however, the efficiency of cleavage varies between domains, and some substrates are domain-specific (*12–14*). The N and C domains of ACE also differ in chloride dependence (*4, 15*) and thermostability (*16*).

These differences between the domains make it appealing to develop an antihypertensive ACE inhibitor therapy that selectively targets one domain. The C domain has been shown to produce the potent vasopressor angiotensin II from angiotensin I more efficiently than the N domain, *in vivo* (*17–19*). Moreover, buildup of bradykinin, a substrate of both domains, has been implicated in a number of ACE

[†] This work was supported by the Wellcome Trust, U.K. (Senior International Research Fellowship 070060 to E.D.S.), the National Research Foundation, South Africa, the Stella and Paul Loewenstein Charitable and Educational Trust, the Ernst and Ethel Erikson Trust, and the University of Cape Town.

[‡] The atomic coordinates and structure factors (entries 3BKK and 3BKL) have been deposited in the Protein Data Bank.

* To whom correspondence should be addressed: Division of Medical Biochemistry, Wernher Beit Building North, University of Cape Town, Observatory 7925, South Africa. Telephone: +2721 406 6312. Fax: +2721 406 6470. E-mail: Edward.Sturrock@uct.ac.za.

[1] Abbreviations: ACE, angiotensin-converting enzyme; SI, sucrase-isomaltase; LPH, lactase-phlorizin hydrolase; kAP, keto-ACE; kAW, (5*S*)-5-[(*N*-benzoyl)amino]-4-oxo-6-phenylhexanoyl-L-tryptophan; kAF, (5*S*)-5-[(*N*-benzoyl)amino]-4-oxo-6-phenylhexanoyl-L-phenylalanine; tACE, testis angiotensin-converting enzyme; tACE-G13, minimally glycosylated tACE mutant; DMSO, dimethyl sulfoxide; HHL, hippuryl-histidyl-leucine; z-FHL, z-phenyl-histidyl-leucine; PDB, Protein Data Bank; CPA, carboxypeptidase A; BOP, 5-amino(*N-tert*-butoxycarbonyl)-2-benzyl-4-oxo-6-phenylhexanoic acid.

10.1021/bi8002605 CCC: $40.75
Published on Web 05/06/2008

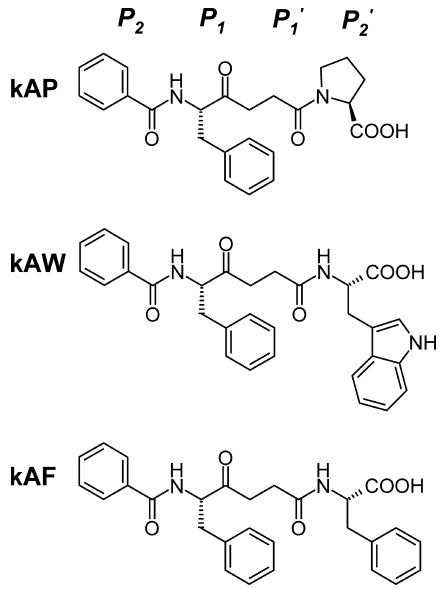

FIGURE 1: Chemical structures of kAP and its derivatives kAW and kAF, showing residue positions relative to the zinc-binding group (P_2, P_1, P_1', P_2').

inhibitor-related side effects (*20–22*). It has been suggested that a C domain-selective ACE inhibitor would reduce blood pressure while allowing the N domain to maintain physiological bradykinin levels, resulting in more effective treatment of hypertension with reduced side effects (*14, 23*).

Keto-ACE (hereafter called kAP), an analogue of the tripeptide ACE inhibitor Bz-Phe-Gly-Pro, has been shown to be 26−34 times more selective for the C domain with a variety of substrates (*24, 25*). Using kAP as a platform and making C-terminal substitutions, our group has synthesized a number of novel compounds. Two of these, (5*S*)-5-[(*N*-benzoyl)amino]-4-oxo-6-phenylhexanoyl-L-tryptophan (kAW) and (5*S*)-5-[(*N*-benzoyl)amino]-4-oxo-6-phenylhexanoyl-L-phenylalanine (kAF) (Figure 1), are highly C domain-selective (*26*).

In this study, we determine the crystal structures of human testis ACE (tACE), which is equivalent to the C domain of ACE, in complex with the novel domain-selective inhibitors kAW and kAF. In addition, we assess the effect of a number of active site mutations on inhibitor binding. This combined structural and kinetic approach allows the determination of the extent to which particular residues contribute to the C domain selectivity of these inhibitors.

EXPERIMENTAL PROCEDURES

tACE Constructs. A fully N-glycosylated tACE mutant, tACEΔ36NJ, truncated after S625 and lacking the 36 O-glycosylated, N-terminal residues (*27*) was cloned into the *Bam*HI and *Eco*RI restriction sites of pcDNA3.1(+) (Invitrogen) for expression purposes. A minimally glycosylated form of this mutant, tACE-G13 (*28*), was used for crystallization.

Inhibitors. Inhibitors kAP, kAW, and kAF were synthesized previously (*26, 29*). Stocks were made by dissolving inhibitors in a small volume of DMSO and then diluting in water or buffer, for enzyme assays.

Cloning and Mutagenesis. Site-directed mutagenesis was performed on an *Sph*I−*Eco*RI fragment of the C domain coding region in pGEM11zf(+) (Promega) as described previously (*30*), converting selected active site residues to their N domain counterparts. Oligonucleotides containing the mutation of interest were synthesized by Inqaba Biotech, and reagents used for site-directed mutagenesis were supplied by Promega. Colonies were screened with appropriate restriction enzymes, and positive clones were confirmed by nucleotide sequencing. C domain mutants were constructed in pcDNA3.1+ for protein expression.

Heterologous Expression and Purification. tACE constructs were expressed in Chinese hamster ovary cells and purified by Sepharose-lisinopril affinity chromatography, as described previously (*28, 31*). ACE activity was detected using a fluorogenic assay with substrates hippuryl-histidyl-leucine (HHL, Sigma) or z-phenyl-histidyl-leucine (z-FHL, Sigma) (*32*). Pooled fractions were dialyzed against 2 L of 0.5 mM Hepes (pH 7.5) overnight. tACE-G13 was concentrated to 1−5 mg/mL for crystallization using an Amicon Ultra-4 spin column (Millipore). The purified protein's molecular weight and purity were assessed using SDS-PAGE.

Crystallization. Crystals were grown by vapor diffusion at 16 °C in hanging drops comprising 2 μL of protein (1.45 mg/mL) or protein/inhibitor solution mixed with 2 μL of reservoir buffer over 1 mL reservoirs covered with 500 μL of oil (3 parts paraffin, 2 parts silicon oil; Hampton) (*33*). Inhibitor-free tACE-G13 microcrystals grew within 2 weeks over reservoirs containing 10 mM sodium acetate (pH 4.7) (Merck), 15% PEG 4000 (Fluka), and 10 μM $ZnSO_4$. Cocrystals of tACE-G13 with inhibitors were grown by streak-seeding these microcrystals into fresh drops containing inhibitor mixed with tACE-G13, over reservoirs containing a higher concentration of sodium acetate (30 mM) but otherwise identical to the reservoirs used for growing microcrystals. Diffracting crystals were grown within 2 weeks in drops containing 1 mM kAW with 1 mg/mL tACE-G13 and 1.25 mM kAF with 1.4 mg/mL tACE-G13.

Data Collection and Processing. Data were collected at 100 K from a single crystal per inhibitor at beamline BM14(UK) of the European Synchrotron Radiation Facility (Grenoble, France) using a wavelength of 1.033 Å.

Data were processed using *HKL2000* (*34*), and phasing was carried out with *EPMR 2.5* (*35*) using protein atoms from the crystal structure of tACE-G13 (PDB entry 2IUL) as a model.

Model building was carried out using *O* version 9.0.7 (*36*), against $2F_{obs} - F_{calc}$, $F_{obs} - F_{calc}$, and composite omit maps (simulated annealing with 5% omission), calculated using *CNS* (*37*). Waters were added using the water_pick protocol of *CNS* (*37*), followed by visual inspection. Ligand molecules were built using *PRODRG* (*38*) and *ARP/wARP* (*39*). Maximum likelihood minimization and simulated annealing of selected residues were carried out using *CNS* (*37*). *PROCHECK* and *SFCHECK* from the *CCP4* program suite (*39*) and *Molprobity* (*40*) were used for model validation. Hydrogen bonds and close contacts were identified using *HBplus* (*41*). Figures were generated using *Pymol* version 0.99 (DeLano Scientific, Palo Alto, CA).

Substrate Hydrolysis. The hydrolysis of the fluorogenic peptide Abz-FRK(Dnp)P-OH (a kind gift from A. Carmona) was characterized in a continuous assay at 25 °C under initial rate conditions, by measuring fluorescence at a λ_{ex} of 320 nm and a λ_{em} of 420 nm. A substrate concentration range of

0−12 μM was added to the reaction mixture of 50 mM Hepes buffer (pH 6.8) containing 200 mM NaCl, 10 μM $ZnCl_2$, and an enzyme concentration of 0.2 nM. Kinetic constants were calculated using the direct linear plot method (*42, 43*).

Inhibition Kinetics. ACE constructs (2 nM) were incubated with an appropriate concentration range of inhibitor in 50 mM Hepes buffer (pH 6.8) containing 200 mM NaCl and 10 μM $ZnCl_2$, at ambient temperature for 60 min. Twenty microliters of the enzyme/inhibitor mixture was added to a reaction mixture of 50 mM Hepes buffer (pH 6.8) containing 200 mM NaCl, 10 μM $ZnCl_2$, and 4 or 8 μM Abz-FRK(Dnp)P-OH, to create a total volume of 300 μL, in triplicate. Residual enzyme activity was monitored by determining the fluorescence at a λ_{ex} of 320 nm and a λ_{em} of 420 nm, at 25 °C. Inhibition constants were calculated using the Dixon method (*44*).

RESULTS

Cocrystal Structures of tACE-G13 with Novel Inhibitors. The C domain-selective compounds kAW and kAF were derived from the moderately domain-selective ketone ACE inhibitor, kAP, by substitution of the P_2' group (Figure 1) (*26, 29*). To understand the mechanism of domain selectivity, we determined cocrystal structures of these two novel inhibitors with tACE, which is identical in sequence to the C domain. To facilitate crystallization, we used a minimally glycosylated construct, tACE-G13, containing only two intact glycosylation sites (*28, 45*). Structures were determined by molecular replacement and refined to final crystallographic *R* factors of 20.0% in both cases. Data processing and refinement statistics are presented in Table 1.

Table 1: X-ray Data Collection and Processing Statistics

	kAW	kAF
resolution (Å)[a]	43−2.18 (2.26−2.18)	43−2.17 (2.25−2.17)
no. of reflections	130768	158385
redundancy[a]	3.8 (3.2)	4.8 (4.1)
completeness (%)[a]	95.0 (95.2)	88.3 (80.2)
$\langle I/\sigma(I)\rangle$[a]	10.87 (2.37)	14.36 (2.61)
no. of molecules per asymmetric unit	1	1
space group	$P2_12_12_1$	$P2_12_12_1$
a (Å)	59.85	60.38
b (Å)	85.04	85.07
c (Å)	134.92	135.51
R_{merge} (%)[a,b]	10.9 (42.1)	8.7 (39.2)
no. of reflections in working set (test set)	31173 (1753)	30340 (1459)
R_{cryst} (%)[a,c]	20.0 (26.6)	20.0 (25.0)
R_{free} (%)[a,d]	23.9 (29.7)	24.3 (26.4)
mean *B* factor (Å^2) (minimum−maximum)	21.6 (2.8−69.0)	22.7 (5.9−72.5)
no. of solvent atoms	254	230
no. of protein atoms[e]	4750	4777
no. of metal ions	3	3
no. of inhibitor atoms	39	36
no. of glycan atoms	67	67
root-mean-square deviations from ideal stereochemistry		
bonds (Å)	0.01	0.01
angles (deg)	1.4	1.3
dihedrals (deg)	22.2	21.2
improper angles (deg)	1.2	1.0
Ramachandran plot, % residues in favored regions	97.40	96.23

[a] Values in parentheses refer to the highest-resolution shell. [b] $R_{merge} = [\sum_h\sum_j|I_j(h) - \langle I(h)\rangle|]/\sum_h\sum_j|I_j(h)|$, where $I_i(h)$ and $\langle I(h)\rangle$ are the *i*th and mean measurements of the intensity of reflection *h*, respectively. [c] $R_{cryst} = \sum_h|F_o - F_c|/\sum_h F_o$, where F_o and F_c are the observed and calculated structure factor amplitudes of reflection *h* of the working set, respectively. [d] R_{free} is equal to R_{cryst} for *h* belonging to the test set of reflections. [e] Excluding duplicated atoms in alternate conformations.

In both the kAW and kAF cocrystal structures, the protein component is in a conformation identical to that of the inhibitor-free tACE-G13 structure (PDB entry 2IUL), as evidenced by all-atom root-mean-square (rms) deviations of 0.61 and 0.67 Å, respectively. Overall, this structure is mostly α-helical and ellipsoid in shape, containing two chloride ions, with the zinc ion buried deep in the active site cleft. As in the unliganded structure, glycan residues are present at the two intact glycosylation sites in tACE-G13, N72 and N109, where there is evidence of glycan-mediated stabilization of the lid helices, as observed previously (*45*).

One inhibitor molecule is bound to the active site of each tACE-G13 molecule, in an extended conformation (Figure 2) similar to that seen for the phosphinic peptide inhibitor, RXPA380 (*46*). Weak density around the P_2' side chain of kAF indicates a degree of flexibility, which is also evidenced by the higher *B* factors of these atoms. These inhibitors have a ketone zinc-binding moiety analogous to the carbonyl oxygen of the scissile peptide bond; however, the density maps surprisingly indicate the stabilization of a hydrated geminal diolate (*gem*-diol) transition state at the active site, in which two oxygens are attached to the carbonyl carbon analogue (Figure 3). The zinc coordination distances for the *gem*-diol oxygens are 2.23 and 2.42 Å for kAW and 2.41 and 2.52 Å for kAF (see Table 1 of the Supporting Information).

kAW makes nine polar contacts (potential hydrogen bonds and ionic interactions) with seven protein side chains, while kAF makes nine polar contacts with six protein side chains, the difference being small changes in the orientations of Q281 and E384 (Table 1 of the Supporting Information). Additional hydrogen bonds are made with four water molecules, the positions of which are conserved between the structures, as well as with a glycerol molecule derived from the cryoprotectant in the kAW structure. The conformation of the Trp moiety of kAW does not appear to be affected by the presence of the glycerol, since it takes the same conformation as the P_2' Trp of RXPA380, which does not have a glycerol in this position. Moreover, no glycerol-like density was present at this position in composite omit maps generated using the RXPA380 structure factors from the Protein Data Bank. These solvent molecules form part of a hydrogen bonding network connecting the inhibitor to other active site residues and to the bulk solvent (Figure 4).

Close contacts are also observed between the nonpolar moieties of the inhibitors and 17 active site residues as well as a number of water molecules (11 and 13 for kAW and kAF, respectively), and glycerol and acetate ions in the case of kAW (Table 2 of the Supporting Information). Some of these active site residues (T282, S355, V379, V380, H387, F457, F512, V518, and F527) could contribute favorably to binding entropy by the hydrophobic effect; others (Q281, H353, A354, E384, D415, and the water molecules) are polar

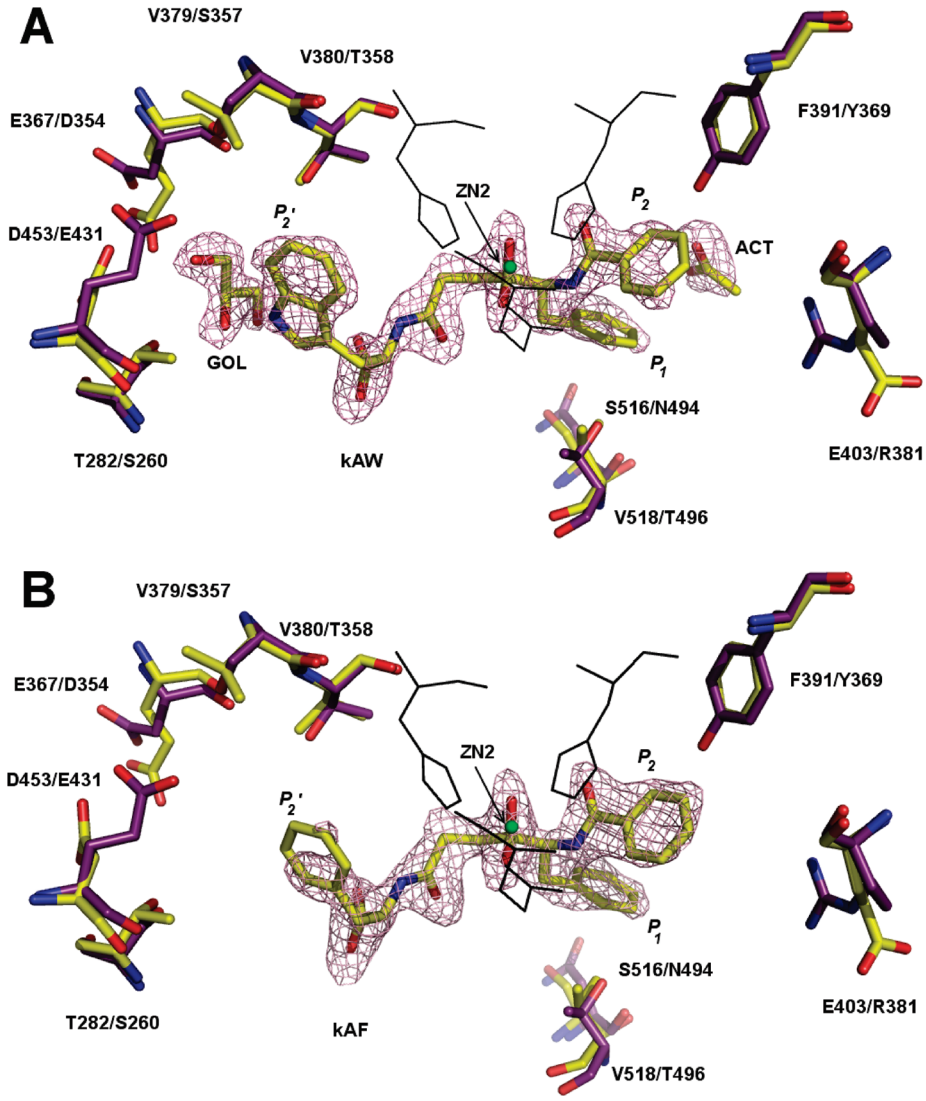

FIGURE 2: Stick representation of kAW (A) and kAF (B) in the active site, showing the first $F_{obs} - F_{calc}$ difference density map (purple mesh) into which the inhibitor model was built, contoured at a level of 3σ. The position of the active site zinc ion (ZN2) is shown as a green nonbonded sphere, indicated with an arrow, and zinc-binding residues are shown as black lines in the foreground. Clear density for a tetrahedral *gem*-diol hydrated form of the zinc-binding ketone moiety is evident. Inhibitor-contacting residues that differ between domains are colored yellow (tACE residues from the cocrystal structure) and purple (N domain residues from the aligned N domain structure; PDB entry 2C6F). Residue labels are given as tACE/N domain, and the P_1, P_2, and P_2' moieties are labeled. In panel A, the active site-associated glycerol (GOL) and acetate (ACT) molecules are also shown as yellow sticks in $F_{obs} - F_{calc}$ difference density.

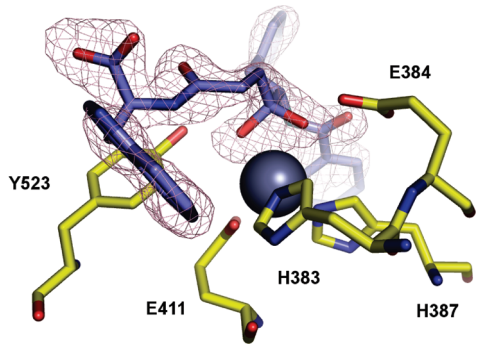

FIGURE 3: Stabilization of the hydrated transition state in the active site. The ketone inhibitor kAW (blue sticks) in $F_{obs} - F_{calc}$ density (purple mesh, contoured at 3σ) has been oriented to show the *gem*-diol moiety coordinating the active zinc ion (gray sphere). The zinc-coordinating residues and those involved in stabilizing the intermediate are labeled and shown as yellow sticks.

or charged groups, and some (H383 and Y523) make both favorable and unfavorable contacts.

Nine residues that interact with kAW and kAF directly, or indirectly via solvent atoms, are replaced with a different amino acid in the N domain and may thus contribute to the domain selectivity of these ketone inhibitors (Figure 2).

Kinetic Analysis of Active Site ACE Mutants. To investigate the role of the nine active site residues that differ between domains, a series of tACE mutants was generated in which these residues were converted to their N domain counterparts (Table 2). All of the mutants had K_m values similar to that of the wild type, and while there was some variation in k_{cat} values, none were significantly lower than that of the wild type (data not shown).

Using the substrate Abz-FRK(Dnp)P-OH under the conditions described here, kAW shows strong C domain selectivity, having almost 1300-fold greater affinity for the C domain than for the N domain (Table 2). The greatest decreases in affinity for kAW observed among the mutants were with the S_1 pocket V518T and S_2 F391Y mutants (Table 2 and Figure 5). The mutants E403R and S516N in these pockets displayed

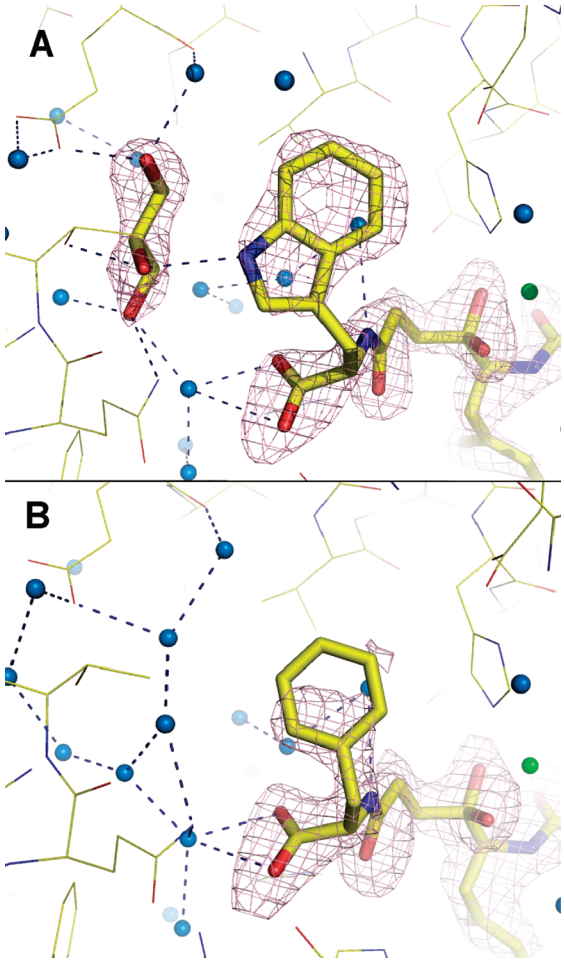

FIGURE 4: Close-up views of the S_2' pocket with kAW (A) and kAF (B), showing the solvent network. The inhibitors and glycerol are shown as yellow sticks in $F_{obs} - F_{calc}$ difference density (purple mesh), contoured at 3σ. The active site zinc ion is shown as a green nonbonded sphere, water molecules are shown as light blue nonbonded spheres, and solvent hydrogen bonds are shown as blue dashed lines.

Table 2: Kinetics of Inhibition by kAW and kAP of tACE Mutants Having Active Site Residues Mutated to Their N Domain Counterparts[a]

pocket	tACE mutant construct[b]	kAW K_i (μM)	kAF K_i (μM)	kAP K_i (μM)
	tACE	0.679	0.83	0.05
S_2'	T282S(260)	0.920	nd[c]	nd[c]
S_2'	E376D(354)	2.33	2.4	nd[c]
S_2'	V379S(357)	0.064	0.81	nd[c]
S_2'	V380T(358)	2.65	1.9	nd[c]
S_2'	V379S/V380T	0.870	nd[c]	nd[c]
S_2'	D453E(431)	0.618	nd[c]	nd[c]
S_1	S516N(494)	0.497	nd[c]	0.012
S_1	V518T(496)	9.74	18.1	1.3
S_2	F391Y(369)	4.75	3.9	0.43
S_2	E403R(381)	0.24	nd[c]	nd[c]
	N domain	854.2	>500	1.5

[a] Inhibition constants were determined using the Dixon method (*44*) with fluorogenic peptide substrate Abz-FRK(Dnp)P-OH. [b] tACE residue and number, followed by the corresponding N domain residue to which it was mutated, with N domain numbering in parentheses. [c] Not determined.

no change in affinity for kAW relative to that of wild-type tACE. In the S_2' pocket, mutants E376D and V380T demonstrated similar increases in K_i, while the V379S mutation caused an increase in affinity for the inhibitor. The

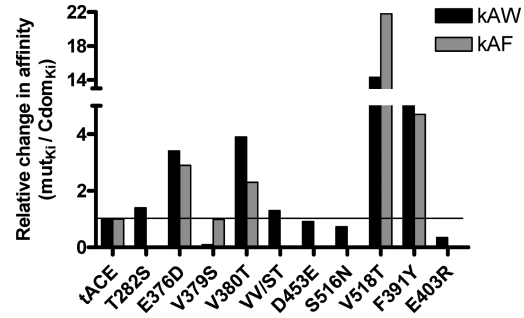

FIGURE 5: Comparison of the relative binding affinity of tACE active site mutants for ketone inhibitors kAW (black bars) and kAF (gray bars) with that of wild-type tACE (C domain). Values above the line represent an N domain-like decrease in affinity relative to that of tACE. The N domain K_i values were 1258- and >602-fold higher than that of tACE for kAW and kAF, respectively.

T282S and D453E mutants displayed K_i values similar to that of the wild-type C domain (Table 2 and Figure 5).

The selectivity of kAW is only 2-fold lower than that of RXPA380, which shares a P_2' Trp, P_1 Phe, and P_2 benzyl moiety with kAW (*14*). However, the affinity of kAW for the C domain is approximately 230-fold lower than that of RXPA380, which has a C domain K_i of 3 nM (*14*). These data for RXPA380 were determined under the same reaction conditions as those used here, but using a different fluorogenic peptide substrate, Mca-ASDK-DpaOH (*14*). No change in selectivity was observed when Abz-FRK(Dnp)P-OH was used (data not shown).

kAF was also shown to be highly C domain-selective under these conditions, with a C domain K_i of 0.83 μM (Table 2). No inhibition of the N domain was observed using up to 500 μM kAF and at a range of chloride concentrations. Because of the limited solubility of this compound, inhibition could not be tested at higher concentrations. The V518T mutation again displayed the greatest decrease in affinity for kAF, while small decreases in affinity were also observed for the F391Y, E376D, and V380T mutants (Table 2 and Figure 5).

To understand the domain selectivity of the parent compound, kAP, we tested the effects of the F391Y, S516N, and V518T mutations in the S_1 and S_2 pockets on the binding affinity of this inhibitor. kAP had a 30-fold higher affinity for the C domain than for the N domain (Table 2). Notably, the F391Y mutation in the S_2 pocket caused an 8-fold decrease in affinity relative to the wild-type C domain, while the S_1 V518T mutant had a K_i similar to that observed for the N domain. The S516N substitution resulted in a binding affinity comparable to that of the wild-type C domain (Table 2).

DISCUSSION

As an enzyme with two homologous catalytically active domains, ACE is an intriguing drug target. Differences in the activity profiles of the domains, particularly with reference to the cleavage of angiotensin I and bradykinin, render it desirable to design selective inhibitors to the C domain; however, the high degree of homology between the domains makes this a complex problem. That domain-selective inhibition is possible is evident from the selectivity of some known substrates and inhibitors, and from the recent identification of the strongly domain-selective phosphinic

peptide inhibitors RXPA380 and RXP407 (*13, 14, 24, 47, 48*). We have recently developed new C domain-selective inhibitors kAW and kAF, based on the moderately domain-selective inhibitor kAP (*26, 29*).

In zinc metalloproteases, peptide bond hydrolysis is thought to occur via a tetrahedral transition state which forms upon nucleophilic attack of the carbonyl carbon by an activated zinc-bound water molecule at the active site (*49, 50*). This is followed by protonation of the scissile amide nitrogen and subsequent peptide bond cleavage. We found that the replacement of the scissile peptide bond nitrogen with a carbon atom in these inhibitors (Figure 1) led to the trapping of the tetrahedral *gem*-diol transition state at the active site (Figure 3).

The hydrated transition state has been observed previously in the structures of carboxypeptidase A (CPA) cocrystallized with ketomethylene inhibitors 5-benzamido-2-benzyl-4-oxopentanoic acid (BOP) and 5-amino(*N-tert*-butoxycarbonyl)-2-benzyl-4-oxo-6-phenylhexanoic acid (*51*, *52*; structures not available in the Protein Data Bank). In these structures, the hydrated form of the ketone was observed at the enzyme active site despite the fact that this form does not occur (<1%) in aqueous solution. Active site stabilization of *gem*-diols is commonly observed in cocrystal structures with aldehyde inhibitors and inhibitors containing activated electrophilic ketones, with examples from the Protein Data Bank including cocrystal structures of leucine aminopeptidase (1LAN) (*53*), CPA (1CBX) (*54*), endothiapepsin (1OD1) (*55*), and human GAR transformylase (1NJS) (*56*). However, the hydration of a ketone in the absence of an activating group, as seen here, has to the best of our knowledge been reported in only two other crystal structures, those of CPA mentioned above.

The *gem*-diol oxygens in the structures of kAW and kAF at the active site of tACE-G13 have partial negative charges and interact with the active site zinc ion (Table 1 of the Supporting Information), in positions similar to those of the carboxyl oxygens of tACE-bound lisinopril and enalaprilat (PDB entries 1O86 and 1UZE). Y523 and E384, which has been proposed to shuttle a proton between the attacking nucleophilic water and the leaving amide, also make hydrogen bonds with the *gem*-diol (Figure 3). In the structure of CPA bound to BOP, the *gem*-diol has longer zinc-coordinating distances [2.51 and 2.91 Å (*51*)] than those observed here; however, it is clear from the overlap of the *gem*-diol oxygens of kAW and kAF with the zinc-binding oxygens of other inhibitors that these positions are characteristic of the ACE active site.

Thus, we have shown that in the absence of a leaving amide nitrogen, the catalytic residues of ACE are able to stabilize the tetrahedral transition state. This stabilization probably plays a transient role in overcoming the energy barrier between substrate and products during catalysis.

The ketone zinc-binding moiety of kAP and its derivative inhibitors has a lower affinity for the active site zinc ion than the carboxyl, sulfydryl, and phosphinyl groups of other previously studied inhibitors (*46, 57, 58*). This results in a situation similar to the binding of a natural substrate, with the affinity of the inhibitor depending to a great extent on the contributions of other groups. These inhibitors are thus suitable tools for investigating the contributions of moieties other than the zinc ion to inhibitor binding.

kAP has a 30-fold higher affinity for the C domain than for the N domain (Table 2). This domain selectivity does not reside in the P_1' position since there is no P_1' side chain in kAP, or in the P_2' moiety, since Pro at this position does not favor binding to one domain (*59*). Moreover, from the cocrystal structures of tACE and the N domain with lisinopril (PDB entries 1O86 and 2C6N, respectively), one can see that a P_2' Pro stacks against Y523 and its N domain equivalent, Y501, making no interactions with residues that differ between domains. Thus, the modest selectivity of kAP must be attributed to its P_1 and P_2 moieties, which are retained in kAW and kAF.

The S_1 and S_2 pockets of the N and C domains differ in four residues that lie within 6 Å of kAW and kAF, of which S516, V518 (S_1 pocket), and F391 (S_2 pocket) make hydrophobic contacts with the inhibitor P_1 and P_2 side chains. These are replaced with the charged and polar residues N494, T496, and Y396, respectively, in the N domain (Figure 2).

Of these substitutions, F391Y and V518T were shown by our kinetic analysis to be important for the selectivity of kAP, reducing affinity 8- and 26-fold, respectively. The F391Y mutation introduces a hydroxyl group into the S_2' pocket, which would result in steric hindrance of the binding of the P_2 benzoyl moiety of kAP. This substitution has been identified as potentially contributing to the C domain selectivity of the phosphinic peptide inhibitor RXPA380, which also has a benzoyl group at this position (*46*).

The effect of the V518T mutation is not steric; however, the association of the P_1 Phe side chain with T496 of the N domain is probably made unfavorable by the displacement of any water molecules hydrogen-bonded to the hydroxyl moiety, which would be necessary for binding of the bulky phenyl group. Displacement of waters around V518, in contrast, would result in a favorable increase in entropy. This S_1 subsite alteration may explain the moderate C domain selectivity of lisinopril and enalaprilat, which also have P_1 phenyl groups, as well as the observation that a bulky P_1 moiety confers C domain selectivity (*60*).

The C domain selectivity of kAP is thus due to sterically and entropically favorable hydrophobic interactions between the bulky hydrophobic P_1 and P_2 benzoyl moieties and F391 and V518, which are replaced with polar groups in the N domain. These substitutions also had a dramatic effect on the binding of kAW and kAF (Figure 5).

The single-residue replacement of Trp for the P_2' Pro of kAP reduces the affinity of kAW for the N domain dramatically, making it approximately 40-fold more C domain-selective than kAP (Table 2). Although the mutation of V518 to Thr did result in a large decrease in affinity for kAW (14-fold), the K_i did not equal that of the N domain, in contrast to the effect observed with kAP, suggesting that other factors play a role in the selectivity of this inhibitor (Table 2).

In the crystal structure, the P_2' Trp indole nitrogen of kAW makes a hydrogen bond to a highly ordered glycerol molecule, which is hydrogen-bonded to T282, Q281, N277, E376, and a network of water molecules in the S_2' subsite (Figure 4). Since this glycerol is derived from the cryoprotectant used for data collection, crystal growth must have occurred in its absence, suggesting that a water molecule was the original acceptor for the Trp hydrogen bond.

In addition to this hydrogen bond, the Trp interacts closely with a hydrophobic patch created by T282, F457, F527, and Y523 on one side and with H383, V379, V380, and a water molecule on the other side (Figure 2 and Table 2 of the Supporting Information). Four of these 10 residues, T282, E376, V379, and V380, are substituted in the N domain (Figure 2).

From the kinetic data, the enhanced selectivity of kAW can be attributed to E376 and V380, with the E376D and V380T mutations demonstrating approximately 4-fold decreases in affinity (Table 2 and Figure 5). Since E376 interacts with the Trp indole N atom indirectly via the glycerol (or water network), the effect of the E376D mutation is probably a result of the weakening of this interaction due to the lengthening of the distance between the negatively charged group and the indole nitrogen. In the N domain structure (PDB entry 2C6F), this side chain is turned away from the active site. The V380T mutation amounts to the introduction of a polar group in proximity to the Trp ring, similar to the S_1 V518T mutation. The overall low affinity of the N domain for kAW is thus probably the combined effect of these two S_2' mutations together with those in the P_1 and P_2 pockets.

Interestingly, the V379S mutant actually displays considerably higher affinity for kAW than the wild type. This effect is not readily explained by the crystal structure but may be due to a rearrangement of side chains in the S_2' pocket, possibly leading to the formation of a water-mediated hydrogen bond between the Ser and the Trp indole N atom. This is supported by the observation that this mutant did not have increased affinity for kAF, which lacks a P_2' hydrogen-bonding moiety (Table 2). The C domain-like affinity of the double VV/ST mutant can be explained as the net result of the affinity-decreasing effect of the V380T mutation and the large affinity-increasing effect of the V379S mutation.

kAF is also strongly C domain-selective, exhibiting no inhibition of the N domain up to 500 μM inhibitor. Like the Trp of kAW, the P_2' side chain contacts V379 and V380, as well as the conserved hydrophobic residues H383, Y523, F527, and F457, but many of these contacts are more distant than those of kAW because of the smaller size of the Phe side chain (Figures 2 and 4 and Table 2 of the Supporting Information). Moreover, the aromatic ring is unable to make a hydrogen bond to the water network, and in place of the glycerol moiety seen in the kAW structure, a ring of ordered waters is present, interacting with the polar residues beyond (Figure 4 and Table 2 of the Supporting Information). The effect of the smaller size of this side chain, together with the lack of a hydrogen-bonding moiety, is evident in the disorder of this group in the crystal structure, in comparison with the Trp of kAW, which displays lower *B* factors and clearer density (Figures 2 and 4).

As with kAW, the mutation of V380 and E376 to T358 and D354, respectively, contributes to the low affinity of this inhibitor for the N domain (Table 2). The selectivity of kAF is thus the combined effect of these mutations, together with the clash of the bulky hydrophobic P_1 and P_2 moieties with F391 and V518.

From this investigation, it can be concluded that the C domain selectivity of the kAP P_2' derivatives kAW and kAF results from interactions between their bulky hydrophobic side chain moieties and the C domain-specific residues F391 (P_2), V518 (P_1), and E376 and V380 (P_2'). Candidate substituted residues T282, V379, E403, D453, and S516 do not individually contribute favorably to the binding of these inhibitors.

It should be noted that the binding affinities of these inhibitors are not of the same order of magnitude as those of currently available drugs such as lisinopril which have K_i values in the low nanomolar range (*60*). Replacing the zinc-binding ketone with another group having a higher affinity for the zinc ion would probably improve the overall affinity; however, this would be a nonselective effect. An approach more suited to domain-selective inhibitor design would be to increase the affinity and selectivity of the inhibitor side chain moieties while maintaining the ketone group. Attention should be paid to increasing the size of the P_2' moiety, since it is evident from the structures that a P_2' Trp or Phe does not fill the pocket sufficiently to take full advantage of all the potential domain-specific contacts. Novel domain-selective effects might also be achieved by introducing a P_1' side chain into these inhibitors.

These data will likely aid in the process of structure-based drug design of domain-selective ACE inhibitors suitable for clinical use, ideally eliminating some of the side effects associated with current ACE inhibitor therapy.

ACKNOWLEDGMENT

We thank Muhammed Sayed and Itai Chitapi for helping with the data collection, Ravi Acharya and Mario Ehlers for helpful comments on the manuscript, and David Christianson for the CPA coordinates.

SUPPORTING INFORMATION AVAILABLE

Polar contacts between the inhibitors kAW and kAF and protein or solvent atoms (Table 1) and nonpolar close contacts between kAW and kAF and protein or solvent atoms, including unfavorable contacts and contacts with waters (Table 2). This material is available free of charge via the Internet at http://pubs.acs.org.

REFERENCES

1. Bergdoll, M., Eltis, L. D., Cameron, A. D., Dumas, P., and Bolin, J. T. (1998) All in the family: Structural and evolutionary relationships among three modular proteins with diverse functions and variable assembly. *Protein Sci. 7*, 1661–1670.
2. Diaz-Mejia, J. J., Perez-Rueda, E., and Segovia, L. (2007) A network perspective on the evolution of metabolism by gene duplication. *Genome Biol. 8*, R26.
3. Soubrier, F., Alhenc-Gelas, F., Hubert, C., Allegrini, J., John, M., Tregear, G., and Corvol, P. (1988) Two putative active centers in human angiotensin I-converting enzyme revealed by molecular cloning. *Proc. Natl. Acad. Sci. U.S.A. 85*, 9386–9390.
4. Wei, L., Alhenc-Gelas, F., Corvol, P., and Clauser, E. (1991) The two homologous domains of human angiotensin I-converting enzyme are both catalytically active. *J. Biol. Chem. 266*, 9002–9008.
5. Erdos, E. G. (1990) Angiotensin-I Converting Enzyme and the Changes in Our Concepts Through the Years: Dahl, Lewis, K. Memorial Lecture. *Hypertension 16*, 363–370.
6. Zaman, M. A., Oparil, S., and Calhoun, D. A. (2002) Drugs targeting the renin-angiotensin-aldosterone system. *Nat. Rev. Drug Discovery 1*, 621–636.
7. Hunziker, W., Spiess, M., Semenza, G., and Lodish, H. F. (1986) The sucrase-isomaltase complex: Primary structure, membrane-orientation, and evolution of a stalked, intrinsic brush border protein. *Cell 46*, 227–234.

8. Mantei, N., Villa, M., Enzler, T., Wacker, H., Boll, W., James, P., Hunziker, W., and Semenza, G. (1988) Complete primary structure of human and rabbit lactase-phlorizin hydrolase: Implications for biosynthesis, membrane anchoring and evolution of the enzyme. *EMBO J. 7*, 2705–2713.
9. Arribas, J. C., Herrero, A. G., Martin-Lomas, M., Canada, F. J., He, S., and Withers, S. G. (2000) Differential mechanism-based labeling and unequivocal activity assignment of the two active sites of intestinal lactase/phlorizin hydrolase. *Eur. J. Biochem. 267*, 6996–7005.
10. Anderson, W. B., and Stadtman, E. R. (1970) Glutamine synthetase deadenylation: A phosphorolytic reaction yielding ADP as nucleotide product. *Biochem. Biophys. Res. Commun. 41*, 704–709.
11. Ellgaard, L., and Ruddock, L. W. (2005) The human protein disulphide isomerase family: Substrate interactions and functional properties. *EMBO Rep. 6*, 28–32.
12. Rousseau, A., Michaud, A., Chauvet, M. T., Lenfant, M., and Corvol, P. (1995) The hemoregulatory peptide N-acetyl-Ser-Asp-Lys-Pro is a natural and specific substrate of the N-terminal active site of human angiotensin-converting enzyme. *J. Biol. Chem. 270*, 3656–3661.
13. Dive, V., Cotton, J., Yiotakis, A., Michaud, A., Vassiliou, S., Jiracek, J., Vazeux, G., Chauvet, M. T., Cuniasse, P., and Corvol, P. (1999) RXP 407, a phosphinic peptide, is a potent inhibitor of angiotensin I converting enzyme able to differentiate between its two active sites. *Proc. Natl. Acad. Sci. U.S.A. 96*, 4330–4335.
14. Georgiadis, D., Beau, F., Czarny, B., Cotton, J., Yiotakis, A., and Dive, V. (2003) Roles of the two active sites of somatic angiotensin-converting enzyme in the cleavage of angiotensin I and bradykinin: Insights from selective inhibitors. *Circ. Res. 93*, 148–154.
15. Wei, L., Clauser, E., Alhenc-Gelas, F., and Corvol, P. (1992) The two homologous domains of human angiotensin I-converting enzyme interact differently with competitive inhibitors. *J. Biol. Chem. 267*, 13398–13405.
16. Voronov, S., Zueva, N., Orlov, V., Arutyunyan, A., and Kost, O. (2002) Temperature-induced selective death of the C-domain within angiotensin-converting enzyme molecule. *FEBS Lett. 522*, 77–82.
17. Junot, C., Gonzales, M. F., Ezan, E., Cotton, J., Vazeux, G., Michaud, A., Azizi, M., Vassiliou, S., Yiotakis, A., Corvol, P., and Dive, V. (2001) RXP 407, a selective inhibitor of the N-domain of angiotensin I-converting enzyme, blocks in vivo the degradation of hemoregulatory peptide acetyl-Ser-Asp-Lys-Pro with no effect on angiotensin I hydrolysis. *J. Pharmacol. Exp. Ther. 297*, 606–611.
18. Fuchs, S., Xiao, H. D., Cole, J. M., Adams, J. W., Frenzel, K., Michaud, A., Zhao, H., Keshelava, G., Capecchi, M. R., Corvol, P., and Bernstein, K. E. (2004) Role of the N-terminal catalytic domain of angiotensin-converting enzyme investigated by targeted inactivation in mice. *J. Biol. Chem. 279*, 15946–15953.
19. Cotton, J., Hayashi, M. A. F., Cuniasse, P., Vazeux, G., Ianzer, D., De Camargo, A. C. M., and Dive, V. (2002) Selective inhibition of the C-domain of angiotensin I converting enzyme by bradykinin potentiating peptides. *Biochemistry 41*, 6065–6071.
20. Nussberger, J., Cugno, M., Amstutz, C., Cicardi, M., Pellacani, A., and Agostoni, A. (1998) Plasma bradykinin in angio-oedema. *Lancet 351*, 1693–1697.
21. Beltrami, L., Zingale, L. C., Carugo, S., and Cicardi, M. (2006) Angiotensin-converting enzyme inhibitor-related angioedema: How to deal with it. *Expert Opin. Drug Saf. 5*, 643–649.
22. Ehlers, M. R. (2006) Safety issues associated with the use of angiotensin-converting enzyme inhibitors. *Expert Opin. Drug Saf. 5*, 739–740.
23. Dickstein, K., and Kjekshus, J. (2002) Effects of losartan and captopril on mortality and morbidity in high-risk patients after acute myocardial infarction: The OPTIMAAL randomised trial. Optimal Trial in Myocardial Infarction with Angiotensin II Antagonist Losartan. *Lancet 360*, 752–760.
24. Deddish, P. A., Marcic, B., Jackman, H. L., Wang, H. Z., Skidgel, R. A., and Erdos, E. G. (1998) N-Domain-specific substrate and C-domain inhibitors of angiotensin-converting enzyme: Angiotensin-(1−7) and keto-ACE. *Hypertension 31*, 912–917.
25. Almquist, R. G., Chao, W. R., Ellis, M. E., and Johnson, H. L. (1980) Synthesis and biological activity of a ketomethylene analogue of a tripeptide inhibitor of angiotensin converting enzyme. *J. Med. Chem. 23*, 1392–1398.
26. Nchinda, A. T., Chibale, K., Redelinghuys, P., and Sturrock, E. D. (2006) Synthesis of novel keto-ACE analogues as domain-selective angiotensin I-converting enzyme inhibitors. *Bioorg. Med. Chem. Lett. 16*, 4612–4615.
27. Yu, X. C., Sturrock, E. D., Wu, Z., Biemann, K., Ehlers, M. R., and Riordan, J. F. (1997) Identification of N-linked glycosylation sites in human testis angiotensin-converting enzyme and expression of an active deglycosylated form. *J. Biol. Chem. 272*, 3511–3519.
28. Gordon, K., Redelinghuys, P., Schwager, S. L., Ehlers, M. R., Papageorgiou, A. C., Natesh, R., Acharya, K. R., and Sturrock, E. D. (2003) Deglycosylation, processing and crystallization of human testis angiotensin-converting enzyme. *Biochem. J. 371*, 437–442.
29. Redelinghuys, P., Nchinda, A. T., Chibale, K., and Sturrock, E. D. (2006) Novel ketomethylene inhibitors of angiotensin I-converting enzyme (ACE): Inhibition and molecular modelling. *Biol. Chem. 387*, 461–466.
30. Papworth, C., Bauer, J. C., Braman, J., and Wright, D. A. (1996) Site-Directed Mutagenesis in One Day with >80% Efficiency. *Strategies 9*, 3–4.
31. Ehlers, M. R., Chen, Y. N., and Riordan, J. F. (1991) Purification and characterization of recombinant human testis angiotensin-converting enzyme expressed in Chinese hamster ovary cells. *Protein Expression Purif. 2*, 1–9.
32. Friedland, J., and Silverstein, E. (1976) A sensitive fluorimetric assay for serum angiotensin-converting enzyme. *Am. J. Clin. Pathol. 66*, 416–424.
33. Chayen, N. E. (1997) The role of oil in macromolecular crystallization. *Structure 5*, 1269–1274.
34. Otwinowski, Z., and Minor, W. (1997) Processing of X-ray diffraction data collected in oscillation mode. *Methods Enzymol. 276*, 307–326.
35. Kissinger, C. R., Gehlhaar, D. K., and Fogel, D. B. (1999) Rapid automated molecular replacement by evolutionary search. *Acta Crystallogr. D55*, 484–491.
36. Jones, T. A. (1978) A graphics model building and refinement system for macromolecules. *J. Appl. Crystallogr. 11*, 268–272.
37. Brunger, A. T., Adams, P. D., Clore, G. M., DeLano, W. L., Gros, P., Grosse-Kunstleve, R. W., Jiang, J. S., Kuszewski, J., Nilges, M., Pannu, N. S., Read, R. J., Rice, L. M., Simonson, T., and Warren, G. L. (1998) Crystallography & NMR system: A new software suite for macromolecular structure determination. *Acta Crystallogr. D54*, 905–921.
38. Schuttelkopf, A. W., and van Aalten, D. M. (2004) PRODRG: A tool for high-throughput crystallography of protein-ligand complexes. *Acta Crystallogr. D60*, 1355–1363.
39. Collaborative Computational Project, No. 4. (1994) The CCP4 suite: Programs for protein crystallography. *Acta Crystallogr. D50*, 760–763.
40. Davis, I. W., Murray, L. W., Richardson, J. S., and Richardson, D. C. (2004) MOLPROBITY: structure validation and all-atom contact analysis for nucleic acids and their complexes. *Nucleic Acids Res. 32*, W615−W619.
41. McDonald, I. K., and Thornton, J. M. (1994) Satisfying hydrogen bonding potential in proteins. *J. Mol. Biol. 238*, 777–793.
42. Eisenthal, R., and Cornish-Bowden, A. (1974) The direct linear plot. A new graphical procedure for estimating enzyme kinetic parameters. *Biochem. J. 139*, 715–720.
43. Carmona, A. K., Schwager, S. L., Juliano, M. A., Juliano, L., and Sturrock, E. D. (2006) A continuous fluorescence resonance energy transfer angiotensin I-converting enzyme assay. *Nat. Protoc. 1*, 1971–1976.
44. Dixon, M. (1953) The determination of enzyme inhibitor constants. *Biochem. J. 55*, 170–171.
45. Watermeyer, J. M., Sewell, B. T., Schwager, S. L., Natesh, R., Corradi, H. R., Acharya, K. R., and Sturrock, E. D. (2006) Structure of testis ACE glycosylation mutants and evidence for conserved domain movement. *Biochemistry 45*, 12654–12663.
46. Corradi, H. R., Chitapi, I., Sewell, B. T., Georgiadis, D., Dive, V., Sturrock, E. D., and Acharya, K. R. (2007) The structure of testis angiotensin-converting enzyme in complex with the C domain-specific inhibitor RXPA380. *Biochemistry 46*, 5473–5478.
47. Hayashi, M. A. F., and Camargo, A. C. M. (2005) The Bradykinin-potentiating peptides from venom gland and brain of *Bothrops jararaca* contain highly site specific inhibitors of the somatic angiotensin-converting enzyme. *Toxicon 45*, 1163–1170.
48. Georgiadis, D., Cuniasse, P., Cotton, J., Yiotakis, A., and Dive, V. (2004) Structural determinants of RXPA380, a potent and highly selective inhibitor of the angiotensin-converting enzyme C-domain. *Biochemistry 43*, 8048–8054.

49. Lipscomb, W. N., and Strater, N. (1996) Recent advances in zinc enzymology. *Chem. Rev. 96*, 2375–2433.
50. Pelmenschikov, V., Blomberg, M. R., and Siegbahn, P. E. (2002) A theoretical study of the mechanism for peptide hydrolysis by thermolysin. *J. Biol. Inorg. Chem. 7*, 284–298.
51. Christianson, D. W., David, P. R., and Lipscomb, W. N. (1987) Mechanism of Carboxypeptidase A: Hydration of a Ketonic Substrate Analogue. *Proc. Natl. Acad. Sci. U.S.A. 84*, 1512–1515.
52. Shoham, G., Christianson, D. W., and Oren, D. A. (1988) Complex between carboxypeptidase A and a hydrated ketomethylene substrate analogue. *Proc. Natl. Acad. Sci. U.S.A. 85*, 684–688.
53. Strater, N., and Lipscomb, W. N. (1995) Transition-State Analog L-Leucinephosphonic Acid Bound to Bovine Lens Leucine Aminopeptidase: X-Ray Structure at 1.65 Angstrom Resolution in a New Crystal Form. *Biochemistry 34*, 9200–9210.
54. Mangani, S., Carloni, P., and Orioli, P. (1992) Crystal structure of the complex between carboxypeptidase A and the biproduct analog inhibitor L-benzylsuccinate at 2.0 Å resolution. *J. Mol. Biol. 223*, 573–578.
55. Coates, L., Erskine, P. T., Mall, S., Williams, P. A., Gill, R. S., Wood, S. P., and Cooper, J. B. (2003) The structure of endothiapepsin complexed with the gem-diol inhibitor PD-135,040 at 1.37 angstrom. *Acta Crystallogr. D59*, 978–981.
56. Zhang, Y., Desharnais, J., Marsilje, T. H., Li, C., Hedrick, M. P., Gooljarsingh, L. T., Tavassoli, A., Benkovic, S. J., Olson, A. J., Boger, D. L., and Wilson, I. A. (2003) Rational design, synthesis, evaluation, and crystal structure of a potent inhibitor of human GAR Tfase: 10-(Trifluoroacetyl)-5,10-dideazaacyclic-5,6,7,8-tetrahydrofolic acid. *Biochemistry 42*, 6043–6056.
57. Natesh, R., Schwager, S. L., Sturrock, E. D., and Acharya, K. R. (2003) Crystal structure of the human angiotensin-converting enzyme-lisinopril complex. *Nature 421*, 551–554.
58. Natesh, R., Schwager, S. L., Evans, H. R., Sturrock, E. D., and Acharya, K. R. (2004) Structural details on the binding of antihypertensive drugs captopril and enalaprilat to human testicular angiotensin I-converting enzyme. *Biochemistry 43*, 8718–8724.
59. Michaud, A., Chauvet, M. T., and Corvol, P. (1999) N-Domain selectivity of angiotensin I-converting enzyme as assessed by structure-function studies of its highly selective substrate, N-acetyl-seryl-aspartyl-lysyl-proline. *Biochem. Pharmacol. 57*, 611–618.
60. Acharya, K. R., Sturrock, E. D., Riordan, J. F., and Ehlers, M. R. (2003) ACE revisited: A new target for structure-based drug design. *Nat. Rev. Drug Discovery 2*, 891–902.

BI8002605